

# 1 **Width of surface rupture zone for thrust earthquakes. Implications** 2 **for earthquake fault zoning.**

3 Paolo Boncio<sup>1</sup>, Francesca Liberi<sup>1</sup>, Martina Caldarella<sup>1</sup>, Fiiia C. Nurminen<sup>2</sup>

4 <sup>1</sup>CRUST-DiSPUTer, “G. D’Annunzio” University of Chieti-Pescara, Chieti, I-66100, Italy

5 <sup>2</sup>Oulu Mining School, University of Oulu, Oulu, FI-90014, Finland

6 *Correspondence to:* Paolo Boncio (paolo.boncio@unich.it)

7 **Abstract.** The characteristics of the zones of coseismic surface faulting along thrust faults are analysed in order  
8 to define the criteria for zoning the Surface Fault Rupture Hazard (SFRH) along thrust faults. Normal and strike-  
9 slip faults have been deeply studied by other authors concerning the SFRH, while thrust faults have not been  
10 studied with comparable attention.

11 Surface faulting data were compiled for 11 well-studied historic thrust earthquakes occurred globally ( $5.4 \leq M \leq$   
12  $7.9$ ). Several different types of coseismic fault scarps characterise the analysed earthquakes, depending on the to-  
13 pography, fault geometry and near-surface materials (simple and hanging wall collapse scarps; pressure ridges;  
14 fold scarps and thrust or pressure ridges with bending-moment or flexural-slip fault ruptures due to large-scale  
15 folding). For all the earthquakes, the distance of distributed ruptures from the principal fault rupture ( $r$ ) and the  
16 width of the rupture zone (WRZ) were compiled directly from the literature or measured systematically in GIS-  
17 georeferenced published maps.

18 Overall, surface ruptures can occur up to large distances from the main fault ( $\sim 2,150$  m on the footwall and  
19  $\sim 3,100$  m on the hanging wall). Most of them occur on the hanging wall, preferentially in the vicinity of the prin-  
20 cipal fault trace ( $> 50\%$  at distances  $< \sim 250$  m). The widest WRZ are recorded where sympathetic slip ( $S_y$ ) on  
21 distant faults occurs, and/or where bending-moment (B-M) or flexural-slip (F-S) fault ruptures, associated with  
22 large-scale folds (hundreds of meters to kilometres in wavelength), are present.

23 A positive relation between the earthquake magnitude and the total WRZ is evident, while a clear correlation be-  
24 tween the vertical displacement on the principal fault and the total WRZ is not found.

25 The distribution of surface ruptures is fitted with probability density functions, in order to define a criterion to  
26 remove outliers (e.g. 90% probability of the cumulative distribution function) and define the zone where the like-  
27 lihood of having surface ruptures is the highest. This might help in sizing the zones of SFRH during seismic mi-  
28 crozonation (SM) mapping.

29 In order to shape zones of SFRH, a very detailed earthquake geologic study of the fault is necessary (the highest  
30 level of SM, i.e., Level 3 SM according to Italian guidelines). In the absence of such a very detailed study (basic  
31 SM, i.e., Level 1 SM of Italian guidelines) a width of ~840 m (90% probability from “simple thrust” database of  
32 distributed ruptures, excluding B-M, F-S and Sy fault ruptures) is suggested to be sufficiently precautionary. For  
33 more detailed SM, where the fault is carefully mapped, one must consider that the highest SFRH is concentrated  
34 in a narrow zone, ~60 m in width, that should be considered as a fault avoidance zone (more than one third of the  
35 distributed ruptures are expected to occur within this zone).

36 The fault rupture hazard zones should be asymmetric compared to the trace of the principal fault. The average  
37 footwall to hanging wall ratio (FW: HW) is close to 1:2.

38 These criteria are applicable to “simple thrust” faults, without considering possible B-M or F-S fault ruptures due  
39 to large-scale folding, and without considering sympathetic slip on distant faults. Areas potentially susceptible to  
40 B-M or F-S fault ruptures should have their own zones of fault rupture hazard that can be defined by detailed  
41 knowledge of the structural setting of the area (shape, wavelength, tightness and lithology of the thrust-related  
42 large-scale folds) and by geomorphic evidence of past secondary faulting. Distant active faults, potentially sus-  
43 ceptible to sympathetic triggering, should be zoned as separate principal faults.

44 The entire database of distributed ruptures (including B-M, F-S and Sy fault ruptures) can be useful in poorly-  
45 known areas, in order to assess the extent of the area within which potential sources of fault displacement hazard  
46 can be present.

47 The results from this study and the database made available as supplementary material can be used for improving  
48 the attenuation relationships for distributed faulting, with possible applications in probabilistic studies of fault  
49 displacement hazard.

## 50 **Key words**

51 Fault rupture hazard, thrust earthquakes, earthquake fault zoning.

## 52 **1 Introduction**

53 Coseismic surface ruptures during large earthquakes might produce damage to buildings and facilities located on  
54 or close to the trace of the active seismogenic fault. This is known as Surface Fault Rupture Hazard (SFRH), a  
55 localized hazard that could be avoided if a detailed knowledge of the fault characteristics is achieved. The mitiga-  
56 tion of SFRH can be faced by strategies of fault zoning and avoidance or, alternatively, by (or together with)

57 probabilistic estimates of fault displacement hazard (e.g. Youngs et al., 2003; Petersen et al., 2011). Both strate-  
58 gies need to employ, as accurately as possible, the location of the active fault trace, the expected displacement on  
59 the principal fault (i.e. *principal faulting* in Youngs et al., 2003; see below for the definition), the deformation  
60 close to the principal fault, and the distribution of other faulting and fracturing away from it (i.e. *distributed fault-*  
61 *ing* in Youngs et al., 2003; see below for the definition). While the general geometry and the expected displace-  
62 ment of the principal fault can be obtained through a detailed geological study and the application of empirical  
63 relationships (e.g. Wells and Coppersmith, 1994), the occurrence of distributed faulting close to and away from  
64 the principal fault rupture is particularly difficult to predict, and only direct observations from well-documented  
65 case studies may provide insights on how distributed faulting is expected to occur (e.g. shape and size of rupture  
66 zones, attenuation relationships for distributed faulting).

67 A reference example of fault zoning strategy for mitigating SFRH is the Alquist-Priolo Earthquake Fault Zoning  
68 Act (A-P Act), adopted by the state of California (USA) in 1972 (e.g. Bryant and Hart, 2007). The A-P Act de-  
69 fines regulatory zones around active faults (Earthquake Fault Zones, EFZ), within which detailed geologic inves-  
70 tigation are required prior to build structures for human occupancy. The boundaries of the EFZ are placed 150-  
71 200 m away from the trace of major active faults, or 60 to 90 m away from well-defined minor faults, with excep-  
72 tions where faults are complex or not vertical. Moreover, the A-P Act defines a minimum distance of 50 feet (15  
73 m) from the well-defined fault trace within which structures designed for human occupancy cannot be built (fault  
74 setback), unless proven otherwise. Similarly, the New Zealand guidelines for development of land on or close to  
75 active faults (Kerr et al., 2003) define a fault avoidance zone to ensure life safety. Fault avoidance zones on dis-  
76 trict planning maps will allow a council to restrict development within the fault avoidance zone and take a risk-  
77 based approach to development in built-up areas. The risk-based approach combines the key elements of fault re-  
78 currence interval, fault complexity and building importance category. The guidelines recommend a minimum  
79 buffer of 20 m either sides of the known fault trace (or the likely rupture zone), unless detailed fault studies prove  
80 that the deformed zone is less than that.

81 Recently, in Italy the Department for Civil Protection published guidelines for land management in areas affected  
82 by active and capable faults. For the purpose of the guidelines, an active and capable fault is defined as a fault  
83 with demonstrated evidence of surface faulting during the last 40,000 years (Technical Commission for Seismic  
84 Microzonation, 2015; SM Working Group, 2015). The guidelines are a tool for zoning active and capable faults  
85 during seismic microzonation (SM). They also contain a number of recommendations to assist land managers and  
86 planners. The fault zones vary at different Levels of SM. In the basic SM (Level 1 SM according to SM Working  
87 Group, 2015), the active fault is zoned with a wide Warning Zone that is conceptually equivalent to the EFZ of

88 the A-P Act. The zone should include all the reasonable inferred fault rupture hazard of both the principal fault  
89 and other secondary faults, and should account for uncertainties in mapping the fault trace. The guidelines rec-  
90 ommend a width of the Warning Zone to be 400 m. Within the Warning Zone, the most detailed level of SM  
91 (Level 3 SM) is recommended; this should be mandatory before new development. Level 3 SM implies a detailed  
92 earthquake geology study of the fault. After completing that study, a new, more accurate fault zoning is achieved.  
93 This includes a 30 m-wide Fault Avoidance Zone around the accurately-defined fault trace. If some uncertainties  
94 persist after Level 3 studies, such as uncertainties about fault trace location or about the possibility of secondary  
95 faulting away from the principal fault, the guidelines suggest the use of a wider zone called Susceptible Zone,  
96 within which development is restricted. Uncertainties within the Susceptible Zone can be reduced by additional  
97 site-specific investigations. The guidelines recommend a width of the Susceptible Zone to be 160 m, but the final  
98 shape and size of the zone depend on the local geology and the level of accuracy reached during Level 3 SM  
99 studies. Both Fault Avoidance and Susceptible Zones can be asymmetric compared with the main fault trace,  
100 with recommended footwall to hanging wall ratios of 1:4, 1:2 and 1:1 for normal, thrust and strike-slip faults, re-  
101 spectively.

102 Shape and width of the zones in the Italian guidelines are based mostly on data from normal faulting earthquakes  
103 (e.g. Boncio et al., 2012). In general, the fault displacement hazard of normal and strike-slip faults (e.g. Youngs  
104 et al., 2003; Petersen et al., 2011) has been much more studied than that of thrust faults. Zhou et al. (2010) ana-  
105 lysed the width of the surface rupture zones of the 2008 Wenchuan earthquake focusing on the rupture zone close  
106 to the principal fault, with implications on the setback distance. However, to our knowledge, a global data compi-  
107 lation from well-documented surface thrust faulting earthquakes aimed at analysing the characteristics of the  
108 WRZ is lacking in the scientific literature.

109 The objectives of this work are: 1) to compile data from well-studied surface faulting thrust earthquakes globally  
110 (we analysed 11 earthquakes with magnitudes ranging from 5.4 to 7.9); 2) to analyse statistically the distribution  
111 of surface ruptures compared to the principal fault and the associated WRZ; and 3) to compare the results with  
112 the Italian guidelines and discuss the implications for earthquake fault zoning.

## 113 **2 Methodology**

114 This work analyses the data from 11 well-studied historic surface faulting thrust earthquakes occurred worldwide  
115 during the last few decades (Table 1). These historic earthquakes range in magnitude ( $M_w$ ) from 5.4 to 7.9 and  
116 belong to different tectonic settings, such as continental collision (Spitak, 1988; Kashmir, 2005; Wenchuan,

117 2008), fold-and-thrust belt (El Asnam, 1980), oceanic-continental or continental-continental collision in large-  
118 scale subduction systems (Chi-Chi, 1999; Nagano, 2014), transform plate boundary (San Fernando, 1971; Coal-  
119 inga-Nunez, 1983) and intraplate regions (Marryat Creek, 1986; Tennant Creek, 1988; Killari, 1993).

120 We compiled from the literature data on both principal and distributed faulting, as defined by Youngs et al.  
121 (2003). Principal faulting is displacement along the main fault responsible for the release of seismic energy dur-  
122 ing the earthquake. At the surface, the displacement may occur along a single narrow trace of the principal fault  
123 or within a meters-scale wide fault zone. Distributed faulting is displacement on other faults in the vicinity of the  
124 principal fault rupture. Distributed ruptures are often discontinuous and may occur tens of meters to kilometers  
125 away from the principal fault rupture. Displacement may occur on secondary faults connected with the principal  
126 fault, such as splay faults, or on pre-existing faults structurally unconnected with the main fault (called here sym-  
127 pathetic fault ruptures). In particular, for the purpose of this work, the following parameters were extracted from  
128 the literature listed in Table 1: i) displacement (vertical, horizontal and net slip, if available) on the principal fault  
129 rupture and coordinates of the referred measurement points for strands of the principal fault having associated  
130 distributed ruptures; ii) distance from the principal fault to the distributed ruptures ( $r$  in Fig. 1), distinguishing be-  
131 tween the ones on hanging wall and on footwall; iii) displacement on distributed ruptures (if available); iv) width  
132 of the rupture zone (WRZ), distinguishing between the ones on hanging wall and on footwall; and v) scarp type  
133 (Fig. 2).

134 When available, the surface rupture data was compiled directly from published tables (e.g., Chi-Chi, 1999; Wen-  
135 chuan, 2008), but in most of the other cases the rupture data was measured from the maps published by the previ-  
136 ous authors that were GIS-georeferenced for the purpose of this work. Figure 1 displays the technique used for  
137 measuring the distance between the principal fault rupture (PF) and the distributed ruptures (DR), which allowed  
138 us to sample the rupture zone systematically and in reasonable detail. The measurements carried out on the pub-  
139 lished maps are illustrated in Fig.s S1 to S11 of the online supplementary material, and the entire compiled data-  
140 base is made available in Table S1. The accuracy of the measurements depends on the scale of the original maps  
141 and on the level of detail reported in the maps (the original scale of the published maps is reported in the figures  
142 of the supplementary material). In this work only detailed maps were considered, and uncertain or inferred rup-  
143 tures were not taken into account. It is important to specify that the database made available in Table S1 of the  
144 supplementary material can be used only for analysing distributed faulting. Data on the principal fault rupture are  
145 not complete, because the strands of the principal fault without distributed ruptures were not considered.

146 In order to distinguish the principal fault rupture from distributed ruptures, all of the following were considered:  
147 1) larger displacement compared to distributed faulting; 2) longer continuity; 3) coincidence or nearly coinci-

148 dence with major tectonic/geomorphologic features, such as the trace of the main fault mapped before the earth-  
149 quake on geologic maps.

150 The distance was measured perpendicularly to the average direction of the principal fault, which was defined by  
151 visual inspection of the published maps, averaging the direction of first-order sections of the principal fault rup-  
152 ture (few to several km-long). Particular attention was paid close to variations of the average strike, in order to  
153 avoid duplicate measurements. In some places, the principal fault rupture is discontinuous. In few of those cases,  
154 and only for the purpose of measuring the distance of distributed ruptures from the main fault trace, we drew the  
155 trace of the main geologic fault between nearby discontinuous ruptures by using major tectonic/geomorphologic  
156 features from available maps (inferred trace of the principal geologic fault in Figs S1, S2, S8, S9, S10 and S11).

157 Distributed ruptures were measured every 200 m along-strike the principal fault. In order to prevent that short  
158 ruptures would be missed or under-sampled during measurement, ruptures shorter than 200 m were measured at  
159 the midpoint, and ruptures between 200 and 400 m-long were measured at the midpoint and endpoints (Fig. 1).

160 Moreover, all the points having displacement information on distributed ruptures were measured. All the points  
161 with displacement values on the principal fault rupture were also measured if distributed ruptures were associated  
162 with that strand of the principal fault. A particular metrics was used for the Sylmar segment of the San Fernando  
163 1971 rupture zone (Fig. S1) where most of the distributed faulting was mapped along roads, resulting in a very  
164 discontinuous pattern of surface ruptures. In order to have a database of measurements statistically equivalent re-  
165 spect to the other studied earthquakes, variable measurement logics were used in order to sample ruptures at dis-  
166 tances that equal more or less 200 m (see Fig. S1 for details).

167 All the distributed ruptures reported in the published maps as of primary (i.e., tectonic) origin were measured.  
168 Only the “Beni Rached” rupture zone of the 1981 El Asnam earthquake (Fig. S2) was not measured. It consists of  
169 normal fault ruptures interpreted to be related to either or both (Yelding et al., 1981; Philip and Meghraoui,  
170 1983): 1) very large gravitational sliding; and 2) surface response of an unconstrained deep tectonic fault also re-  
171 sponsible for the 1954 M 6.7 earthquake. Therefore, we avoided measuring the rupture due to the large uncertain-  
172 ties concerning its primary origin.

173 Some distributed ruptures reasonably unconnected with the main seismogenic fault were classified as sympathet-  
174 ic fault ruptures (Sy; Figs. S1, S2 and S5). We included in this category a rupture on a pre-existing thrust fault  
175 located more than 2 km in the hanging wall of the Chi-Chi 1999 principal fault rupture, due to its large distance  
176 from the main fault trace compared to all the other distributed ruptures (Tsauton East fault, Fig. S8), but a deep  
177 connection with the main seismogenic fault is possible (Ota et al., 2007a).

178 The measured ruptures have been classified according to the scarp types illustrated in Fig. 2, alternatively the  
179 scarp type was classified as “Unknown”. Scarp types from “a” to “g” (Fig. 2) follow the scheme proposed by  
180 Philip et al. (1992), integrated with the classification of Yu et al. (2010). In case of steeply dipping faults, a sim-  
181 ple thrust scarp in bedrock (type a) or a hanging wall collapse scarp in bedrock or in brittle unconsolidated mate-  
182 rial (type b) are produced. In case of low-angle faults and presence of soft-sediment covers, various types of pres-  
183 sure ridges (types c to f) can be observed, depending on the displacement, sense of slip and behaviour of near-  
184 surface materials. In presence of shallow blind faults, a fault-related fold scarp may be formed (type g). Moreo-  
185 ver, in this study two additional structural contexts were distinguished, which are characterized by the occurrence  
186 of bending-moment and flexural-slip fault ruptures (Yeats, 1986), associated with large-scale folds (hundreds of  
187 meters to kilometres in wavelength). Both of these occurred widely during the 1980 El Asnam earthquake (Philip  
188 and Meghraoui, 1983). Bending-moment faults (type h in Fig. 2) are normal faults that are formed close to the  
189 hinge zone of large-scale anticlines (extensional faults at the fold extrados in Philip and Meghraoui, 1983), while  
190 flexural-slip faults (type i) are faults that are formed due to differential slip along bedding planes on the limbs of  
191 a bedrock fold. Bending-moment distributed ruptures associated with small-scale folds (meters to dozens of me-  
192 ters in wavelength), which form at the leading edge of the thrust, belong to scarp types “c” to “g”.

### 193 **3 Width of the Rupture Zone (WRZ): statistical analysis**

194 The most impressive and recurrent measured features are ruptures occurring along pre-existing fault traces and on  
195 the hanging wall, as the result of the reactivation of the main thrust at depth. Distributed ruptures are mainly rep-  
196 resented by synthetic and antithetic faults, which are parallel to or branching from the main fault. Fault segmenta-  
197 tion and en échelon geometries are common in transfer zones or in oblique-slip earthquakes.

198 The collected data was analysed in order to evaluate the width of the rupture zone (WRZ), intended as the total  
199 width, measured perpendicularly to the principal fault rupture, within which all the distributed ruptures occur.  
200 Figure 3 shows frequency distribution histograms of the distance of distributed ruptures from the principal fault  
201 ( $r$ ) for all the analysed earthquakes. Negative values refer to the footwall, while positive values refer to the hang-  
202 ing wall. In particular, in Fig. 3a we distinguished the scarps with bending-moment (B-M), flexural-slip (F-S) or  
203 sympathetic (Sy) fault ruptures from the other types; in Fig. 3b the scarps without B-M, F-S or Sy fault ruptures  
204 are distinguished by scarp types, and in Fig. 3c the scarps with B-M, F-S or Sy fault ruptures are distinguished by  
205 earthquake. In general, although the values span over a large interval (-2,150 m in the footwall; 3,100 m in the

206 hanging wall), most of them occur in the proximity of the principal fault and display an asymmetric distribution  
207 between hanging wall and footwall.

208 In Fig. 3b all the data (excluding scarps with B-M, F-S and Sy fault ruptures) are distinguished by scarp type.  
209 Simple Pressure Ridges with narrow WRZ prevail. Larger WRZ characterizes back-thrust, low-angle and oblique  
210 pressure ridges, implying that the main thrust geometry, the local kinematics and the near-surface rheology have  
211 a significant control in strain partitioning with consequences on the WRZ, as expected.

212 The occurrence of B-M or F-S fault ruptures is strictly related to the structural setting of the earthquake area. In  
213 particular, B-M fault ruptures, which are related to the presence of large-scale hanging wall anticlines, were  
214 clearly observed in the El Asnam 1980 (Philip and Meghraoui, 1983) and Kashmir 2005 (southern part of central  
215 segment; Kaneda et al., 2008; Sayab and Khan, 2010) earthquakes. A wide extensional zone (1.8 km-long in the  
216 E-W direction; 1.3 km-wide) formed on the eastern hanging wall side of the Sylmar segment of the San Fernando  
217 1971 surface rupture. The interpretation of such an extensional zone is not straightforward. Nevertheless, the  
218 presence of a macro-anticline in the hanging wall of the Sylmar fault is indicated by subsurface data (Mission  
219 Hill anticline; Tsutsumi and Yeats, 1999). Though it is not possible to clearly classify these structures as B-M  
220 faults in strict sense, it seems reasonable to interpret them as generic fold-related secondary extensional faults.  
221 Therefore, they were plotted in Fig.s 3a and 3c together with B-M fault ruptures. F-S fault ruptures were ob-  
222 served on the upright limb of a footwall syncline in the El Asnam 1980 earthquake.

223 Ruptures close to the main fault ( $r < 150$  m) are due to processes operating in all the scarp types (Fig. 3b), but for  
224 larger distances the distributed faulting can be affected by other processes such as large-scale folding or sympa-  
225 thetic reactivation of pre-existing faults (Fig.s 3a and 3c), contributing significantly in widening the WRZ.

226 For the analysis of the statistical distribution of “r”, the collected data was fitted with a number of probability  
227 density functions by using the commercial software EasyFitProfessional©V.5.6 (<http://www.mathwave.com>),  
228 which finds the probability distribution that best fits the data and automatically tests the goodness of the fitting.  
229 We decided to analyse both the database without B-M, F-S and Sy fault ruptures (called here “simple thrust” dis-  
230 tributed ruptures; Fig. 4) and the entire database of distributed ruptures without filtering (Fig. 5). The aim is to  
231 analyse separately: 1) distributed ruptures that can be reasonably related only to (or preferentially to) the coseis-  
232 mic propagation to the ground surface of the main fault rupture; they are expected to occur in a rather systematic  
233 way compared to the main fault trace; and 2) distributed ruptures that are affected also by other, non-systematic  
234 structural features, mostly related to large-scale coseismic folding. The hanging wall and footwall data were fitted  
235 separately and the results are synthesized in Fig.s 4 and 5, where the best fitting distribution curves and the cumu-  
236 lative curves are shown.

237 For “simple thrust” distributed ruptures, the hanging wall data (Figs. 4a and 4b) has a modal value of 7.1 m. The  
238 90% probability (0.9 of the cumulative distribution function, HW90) seems to be a reasonable value to cut off the  
239 outliers (flat part of the curves). It corresponds to a distance of ~575 m from the principal fault. From a visual in-  
240 spection of the histogram (Fig. 4b), there is an evident sharp drop of the data approximately at the 35% probabili-  
241 ty (HW35), corresponding to a distance of ~40 m from the principal fault. The second sharp drop of the data in  
242 the histogram occurs close to the 50% probability (HW50, corresponding to ~80 m from the principal fault). Also  
243 the 3rd quartile is shown (HW75), corresponding to a distance of ~260 m from the main fault. The widths of the  
244 zones for the different probabilities (90%, 75%, 50% and 35%) are listed in Table 2a.

245 The footwall data (Figs. 4c and 4d) has a modal value of the best fitting probability density function of 5 m. By  
246 applying the same percentiles used for the hanging wall, a 90% cut off (FW90) was found at a distance of ~265  
247 m from the principal fault. The FW75, FW50 and FW35 correspond to distances of ~120 m, ~45 m and ~20 m  
248 from the principal fault, respectively (Table 2a). It is worth noticing that also for the footwall the 35% probability  
249 corresponds to a sharp drop of the data.

250 The ratio between the width of the rupture zone on the footwall and the width of the rupture zone on the hanging  
251 wall ranges from 1:1.8 to 1:2.2 (Table 2a), and therefore it is always close to 1:2 independently from the used  
252 percentile.

253 The results of the analysis performed on the entire database of distributed ruptures, including also the more com-  
254 plex secondary structures of B-M, F-S and Sy fault ruptures, is illustrated in Fig. 5 and summarized in Table 2b.  
255 As expected, the WRZ is significantly larger than for “simple thrust” distributed ruptures. The HW90, HW75 and  
256 HW50 correspond to distances of ~1100 m, ~640 m and ~260 m from the principal fault, respectively. For com-  
257 parison with the “simple thrust” distributed ruptures, also the HW35 was calculated (~130 m), but it does not cor-  
258 respond with a particular drop of the data in the histogram of Fig. 5b. Instead, a sharp drop is visible at a distance  
259 of ~40 m from the principal fault, as for the “simple thrust” database. In the footwall, the FW90, FW75 and  
260 FW50 correspond to distances of ~720 m, ~330 m and ~125 m from the principal fault, respectively. The FW35  
261 corresponds to a distance of ~65 m, but the sharp drop of the data in the histogram of Fig. 5d is at a distance of  
262 ~20 m from the principal fault, as for the “simple thrust” database.

263 In order to analyse the potential relationships between WRZ and the earthquake size, in Fig. 6 the total width of  
264 the rupture zone ( $WRZ_{tot} = WRZ_{hanging\ wall} + WRZ_{footwall}$ ) is plotted against  $M_w$  (Fig. 6a) and, for the  
265 subset of data having displacement information, against the vertical displacement (VD) on the principal fault  
266 (Fig. 6b). The vertical displacement measured at the ground surface is highly sensitive to the shallow geometry of  
267 the thrust plane. The net displacement along the slip vector is a more appropriate parameter for considering the

268 size of the displacement at the surface. However, the net displacement is rarely given in the literature, or can be  
269 obtained only by assuming a fault dip, while VD is the most commonly measured parameter. Therefore, we used  
270 VD as a proxy of the amount of surface displacement. In Fig. 6a a positive relation between the total WRZ and  
271 Mw is clear, particularly if sympathetic (Sy) fault ruptures are not considered. In fact, Sy data appear detached  
272 from the other data, suggesting that their occurrence is only partially dependent on the magnitude of the  
273 mainshock. They also depend on the structural features of the area, such as 1) whether or not an active, favoura-  
274 bly-oriented fault is present, and 2) its distance from the main seismogenic source. A correlation between the to-  
275 tal WRZ and VD is not obvious (Fig. 6b). Even for small values of VD ( $< 1$  m) the total WRZ can be as wide as  
276 hundreds of meters, but a larger number of displacement data is necessary for drawing convincing conclusions.

#### 277 **4 Comparison with Italian guidelines and implications for fault zoning during seismic microzonation**

278 The definition of the WRZ based on the analysis of the data from worldwide thrust earthquakes can support the  
279 evaluation and mitigation of SFRH. The values reported in Table 2 can be used for shaping and sizing fault zones  
280 (e.g. Warning or Susceptible Zones in the Italian guidelines; Earthquake Fault Zones in the A-P Act) and avoid-  
281 ance zones around the trace of active thrust faults (Table 3).

282 A first question that needs to be answered is which set of data between “simple thrust” distributed ruptures (Fig.  
283 4; Table 2a) and all distributed ruptures (Fig. 5, Table 2b) is the most appropriate to be used for sizing the fault  
284 zones. The answer is not easy and implicates some subjective choices. In Table 3 we suggest using the results  
285 from “simple thrust” distributed ruptures. The results from all distributed ruptures can be used in areas with poor  
286 geologic knowledge, in order to assess the extent of the area within which potential sources of fault displacement  
287 hazard can be present. Our choices result from the following line of reasoning:

288 1) The data analysed in this work are from brittle rupture of the ground surface. The measured distributed rup-  
289 tures are always associated with surface faulting on the principal fault. Therefore, the results can be used for zon-  
290 ing the hazard deriving from mechanisms connected with the propagation of the rupture on the main fault plane  
291 up to the surface. Deformations associated with blind thrusting are not analysed. Therefore, the results are not  
292 suitable for zoning ductile tectonic deformations associated with blind thrusting (e.g. folding). Clearly, coseismic  
293 folding occurs both during blind thrusting and surface faulting thrusting. Furthermore, brittle surface ruptures and  
294 other ductile deformations can be strictly connected to each other, making difficult to separate the two compo-  
295 nents, but a global analysis of the entire spectrum of permanent tectonic deformation associated to thrust faulting  
296 need additional data not considered here.

297 2) In most cases, distributed ruptures occur on secondary structures that are small and cannot be recognized be-  
298 fore the earthquake, or that only site-specific investigations could distinguish. Fault zones should include the haz-  
299 ard from this kind of ruptures.

300 3) Some secondary faults connected with the principal fault can be sufficiently large to have their own geologic  
301 and geomorphic signature, and can be recognized before the earthquake. Most likely, close to the surface these  
302 structures behave similarly to the principal fault, with their own distributed ruptures. Faults with these character-  
303 istics should have their own zone, unless they are included in the principal fault zone.

304 4) Point 3 also applies to distant large active faults that can undergo sympathetic triggering. They should be  
305 zoned as separate principal faults. Using Sy fault ruptures for shaping zones of fault rupture hazard would imply  
306 distributing the hazard within areas that can be very large (Fig.s 5, 6). The size of the resulting zone would de-  
307 pend mostly on the structural setting of the analysed areas (presence or not of the fault, distance from the seismo-  
308 genic source) rather than the mechanics which controls distributed faulting in response to principal faulting.

309 5) B-M and F-S fault ruptures are not always present. Where present, they occur over distances ranging from  
310 hundreds of meters to kilometers (Fig. 3c). In any case, B-M and F-S secondary faults are strictly related to the  
311 structural setting of the area (large-scale folding; fold shape, wavelength and tightness; stiffness of folded strata).  
312 In fact, B-M fault ruptures commonly observed in historical earthquakes are normal faults. B-M normal faults are  
313 expected to occur in the shallowest convex (lengthened) layer of the folded anticline. They can occur only where  
314 the bending stress is tensional, that is the convex side of the folded layer, preferentially close to the crest of the  
315 anticline and parallel to the anticline hinge. F-S faults can rupture the surface where the steeply-dipping limb of a  
316 fold is formed by strata of stiff rocks able to slip along bedding planes (e.g. Fig. 2i). Moreover, it is known that  
317 coseismic B-M or F-S faults often reactivate pre-existing fault scarps (e.g. Yeats, 1986) which might help in zon-  
318 ing the associated potential fault rupture hazard before the earthquake. Therefore, knowledge of the structural set-  
319 ting of the area can help in identifying zones potentially susceptible to B-M or F-S faulting, which should be  
320 zoned as separate sources of fault rupture hazard.

321  
322 In Table 3, the total WRZ from the present study is compared with the sizes of the zones proposed by the Italian  
323 guidelines for SM studies (Technical Commission for Seismic Microzonation, 2015; SM Working Group, 2015).  
324 The values reported in Table 3 could be used for integrating the existing criteria. In particular, the total WRZ  
325 from “simple thrust” distributed ruptures is used for sizing Warning Zones (Level 1 SM) and Susceptible and  
326 Avoidance Zones (Level 3 SM). The total WRZ from all distributed ruptures is suggested to be used for sizing  
327 Warning Zones in areas with poor basic geologic knowledge (Level 1 SM).

328 The first observation is that the FW:HW ratio proposed by the Italian guidelines is supported by the results of this  
329 study (FW:HW ratio close to 1:2).

330 Assuming that the 90% probability is a reasonable criterion for cutting the outliers from the analysed population,  
331 the resulting total WRZ (HW + FW) for “simple thrust” distributed ruptures is 840 m (560 m on the HW + 280 m  
332 on the FW). This width could be used for zoning all the reasonably inferred fault rupture hazard, from both the  
333 principal fault and distributed ruptures, during basic (Level 1) SM studies, which do not require high-level specif-  
334 ic investigations. The obtained value is significantly different from that recommended by the Italian guidelines  
335 for Level 1 SM (400 m).

336 A significant difference between our proposal and the Italian guidelines concerns also the width of the zone that  
337 should be avoided, due to the very high likelihood of having surface ruptures. Though the entire rupture zone  
338 could be hundreds of meters wide, more than one third of distributed ruptures are expected to occur within a nar-  
339 row, 60 m-wide zone. As could be expected, only site-specific paleosismologic investigations can quantify the  
340 hazard from surface faulting at a specific site. In the absence of such a detail, and for larger areas (e.g. municipal-  
341 ity scale) the fault avoidance zone should be in the order of 60 m, shaped asymmetrically compared to the trace  
342 of the main fault (40 m on the HW; 20 m on the FW).

343 In Table 3 a width of 380 m is proposed for the susceptible zone (Level 3 SM). The choice of defining the width  
344 of the zone as the 3rd quartile (3 out of 4 probability that secondary faulting lies within the zone) is rather arbi-  
345 trary. In fact, the width of the susceptible zone should be flexible. Susceptible zones are used only if uncertainties  
346 remain also after high-level seismic microzonation studies, such as uncertainties on the location of the main fault  
347 trace or about the possibility of secondary faulting away from the main fault. Susceptible zones can also be used  
348 for areas where a not better quantifiable distributed faulting might occur, such as in structurally complex zones  
349 (e.g. stepovers between main fault strands).

350 **5 Conclusions**

351 The distribution of coseismic surface ruptures (distance of distributed ruptures from the principal fault rupture)  
352 for 11 well-documented historical surface faulting thrust earthquakes ( $5.4 \leq M \leq 7.9$ ) provide constraints on the  
353 general characteristics of the surface rupture zone, with implications for zoning the surface rupture hazard along  
354 active thrust faults.

355 Distributed ruptures can occur up to large distances from the principal fault (up to ~3,000 m on the hanging wall),  
356 but most of them occur within few dozens of meters from the principal fault. The distribution of secondary rup-

357 tures is asymmetric, with most of them located on the hanging wall. Coseismic folding of large-scale folds (hun-  
358 dreds of meters to kilometres in wavelength) may produce bending-moment (B-M) or flexural-slip (F-S) fault  
359 ruptures on the hanging wall and footwall, respectively, widening significantly the rupture zone. Additional wid-  
360 ening of the rupture zone can be due to sympathetic slip on distant active faults (Sy fault ruptures).

361 The distribution of secondary ruptures for “simple thrust” ruptures (without B-M, F-S, and Sy fault ruptures) can  
362 be fitted by a continuous probability density function, of the same form for both the hanging wall and footwall.  
363 This function can be used for removing outliers from the analysed database (e.g. 90% probability) and define cri-  
364 teria for shaping SFRH zones. These zones can be used during seismic microzonation studies and can help in in-  
365 tegrating existing guidelines. More than one third of the ruptures are expected to occur within a zone of ~60 m  
366 wide. This narrow zone could be used for defining the fault avoiding zone during high-level, municipality-scale  
367 seismic microzonation studies (i.e. Level 3 SM according to the Italian guidelines). The average FW:HW ratio of  
368 the WRZ is close to 1:2, independently from the used percentile.

369 In addition to the expected rupture zone along the trace of the main thrust, zones potentially susceptible to B-M  
370 or F-S secondary faulting can be identified by detailed structural study of the area (shape, wavelength, tightness  
371 and lithology of the thrust-related large-scale folds) and by scrutinize possible geomorphic traces of past second-  
372 ary faulting. Where recognized, these areas should have their own zones of fault rupture hazard.

373 The analysis of the entire database of distributed ruptures (Fig. 5) indicates significantly larger rupture zones  
374 compared to the database without B-M, F-S and Sy fault ruptures. This is due to the combination of processes re-  
375 lated to the propagation up to the surface of the main fault rupture and other processes associated with large-scale  
376 coseismic folding, as well as triggering of distant faults. These data can be useful in poorly-known areas, in order  
377 to assess the extent of the area within which potential sources of fault displacement hazard can be present.

378 The results from this study, particularly the function obtained in Fig. 4, can be used for improving the attenuation  
379 relationships for distributed faulting with distance from the principal fault, with possible applications in probabil-  
380 istic studies of fault displacement hazard (e.g., Youngs et al., 2003; Petersen et al., 2011).

### 381 **Competing interests**

382 The authors declare that they have no conflict of interest.

383 **Acknowledgements**

384 The project was funded by Department DiSPUTer, “G. D’Annunzio” University of Chieti-Pescara (research  
385 funds to P. Boncio).

387 **References**

388 Angelier, J., Lee, J. C., Chu, H. T., and Hu, J. C.: Reconstruction of fault slip of the September 21st, 1999, Tai-  
389 wan earthquake in the asphalted surface of a car park, and co-seismic slip partitioning, *J. Struct. Geol.*, 25,  
390 345-350, 2003.

391 Avouac, J. P., Ayoub, F., Leprince, S., Konea, O., and Helmberger, V.: The 2006 Mw 7.6 Kashmir earthquake:  
392 sub-pixel correlation of ASTER images and seismic waveforms analysis, *Earth Planet. Sci. Lett.*, 249, 514-  
393 528, 2006.

394 Bilham, R. and Yu, T. T.: The morphology of thrust faulting in the 21 September 1999, Chichi, Taiwan earth-  
395 quake, *J. Asian Earth Sci.*, 18, 351-367, 2000.

396 Boncio, P., Galli, P., Naso, G., and Pizzi, A.: Zoning Surface Rupture Hazard along Normal Faults: Insight from  
397 the 2009 M<sub>w</sub> 6.3 L’Aquila, Central Italy, *Earthquake and Other Global Earthquakes*, *Bull. Seism. Soc. Am.*,  
398 102, 918-935, doi: 10.1785/0120100301, 2012.

399 Bowman, J. R. and Barlow, B. C.: Surveys of the fault scarp of the 1986 Marryat Creek, South Australia, earth-  
400 quake, [Australian] Bureau of Mineral Resources, *Geology and Geophysics Record* 1991/190, 12 pp., 3 plates,  
401 1991.

402 Bryant, W. A. and Hart, E. W.: Fault-Rupture Hazard Zones in California, *Alquist-Priolo Earthquake Fault Zon-*  
403 *ing Act With Index to Earthquake Fault Zones Maps*, *Calif Geol. Surv. Spec. Pub.*, 42, 41 pp, 2007.

404 Central Geological Survey, MOEA at <http://gis.moeacgs.gov.tw/gwh/gsb97-1/sys8/index.cfm>

405 Chang, J. C. and Yang, G. S.: Deformation and occurrence of the Che-lung-pu Fault from geomorphic evidence,  
406 *Quat. Int.*, 115-116, 177-188, 2004.

407 Chen, C. H., Chou, H.S., Yang, C.Y., Shieh, B. J., and Kao, Y. H.: Chelungpu fault inflicted damages of pile  
408 foundations on FWY rout 3 and Fault zoning regulations in Taiwan, *A Workshop on Seismic Fault-induced*  
409 *Failures*, Tokyo, 2003.

410 Chen, G. H., Xu, X. W., Zheng, R. Z., Yu, G. H., Li, F., Li, C. X., Wen, X. Z., He, Y. L., Ye, Y. Q., Chen, X. C.,  
411 and Wang, Z. C.: Quantitative analysis of the co-seismic surface rupture of the 2008 Wenchuan earthquake,

412 Sichuan, China along the Beichuan-Yingxiu Fault, *Seismol. Geol.*, 30 (3), 723-738, 2008 (in Chinese with  
413 English abstract).

414 Chen, W. C., Chu, H. T., and Lai, T. C.: Surface ruptures of the Chi-Chi Earthquake in the Shihgang Dam area,  
415 Special Issue for the Chi-Chi Earthquake, 1999, Special Publication of the Central Geological Survey, 12, 41-  
416 62, 2000 (in Chinese with English abstract).

417 Crone, A. J., Machette, M. N., and Bowman, J. R.: Geologic investigations of the 1988 Tennant Creek, Australia,  
418 earthquakes— Implications for paleoseismicity in stable continental regions, *U.S. Geol. Surv. Bull.* 2032-A,  
419 A1–A51, 1992.

420 Dong S, Zhang Y, Wu Z, Yang, N., Ma, Y., Shi, W., Chen, Z., Long, C., and An, M.: Surface Rupture and Co-  
421 seismic Displacement Produced by the Ms8.0 Wenchuan Earthquake of May 12th, 2008, Sichuan, China:  
422 Eastwards Growth of the Qinghai-Tibet Plateau, *Acta Geol. Sin.*, 82 (5), 938-948, 2008a.

423 Dong, S., Han, Z., and An, Y.: Surface deformation at the epicenter of the May 12, 2008 Wenchuan M8 Earth-  
424 quake, at Yingxiu Town of Sichuan Province, China, *Sci. China Ser. E*, 51, 154–163, doi:10.1007/s11431-  
425 008-6007-0, 2008b.

426 Faccioli, E., Anastasopoulos, I., Gazetas, G., Callerio, A., and Paolucci R.: Fault rupture–foundation interaction:  
427 selected case histories, *Bull. Earthquake Eng.*, 6 (4), 557-583, 2008.

428 Fredrich, J., McCaffrey, R., and Denham, D.: Source parameters of seven large Australian earthquakes deter-  
429 mined by body waveform inversion, *Geoph. J.*, 95, 1-13, 1988.

430 Haessler, H., Deschamps, A., Dufumier, H., Fuenzalida, H. and Cisternas, A.: The rupture process of the Arme-  
431 nian earthquake from broad-band teleseismic body wave records, *Geophys. J. Int.*, 109, 151-161, 1992.

432 Huang, C., Chan, Y. C., Hu, J. C., Angelier, J., and Lee, J. C.: Detailed surface co-seismic displacement of the  
433 1999 Chi-Chi earthquake in western Taiwan and implication of fault geometry in the shallow subsurface, *J.*  
434 *Struct. Geol.*, 30, 1167-1176, 2008.

435 Huang, W. J., Chen, Z. Y., Liu, S. Y., Lin, Y. H., Lin, C. W., and Chang, H. C.: Surface deformation models of  
436 the 1999 Chi–Chi earthquake between Tachiachi and Toupienkengchi, central Taiwan, Special Issue for the  
437 Chi-Chi Earthquake, 1999, Special Publication of the Central Geological Survey, 12, 63–87, 2000 (in Chinese  
438 with English abstract).

439 Huang, W. J.: Deformation at the leading edge of thrust faults, Ph.D. dissertation, Purdue University, West Lafa-  
440 yette, Indiana, 435 pp., 2006.

- 441 Ishimura, D., Okada, S., Niwa, Y., and Toda, S.: The surface rupture of the 22 November 2014 Nagano-ken-  
442 hokubu earthquake (Mw 6.2), along the Kamishiro fault, Japan, *Active Fault Research*, 43, 95-108, 2015 (in  
443 Japanese with English abstract).
- 444 Kaneda, H., Nakata, T., Tsutsumi, H., Kondo, H., Sugito, N., Awata, Y., Akhtar, S. S., Majid, A., Khattak, W.,  
445 Awan, A. A., Yeats, R. S., Hussain, A., Ashraf, M., Wesnousky, S. G. and Kausar, A. B.: Surface rupture of  
446 the 2005 Kashmir, Pakistan, Earthquake and its active tectonic implications, *Bull. Seismol. Soc. Am.*, 98,  
447 521–557, 2008.
- 448 Kawashima, K.: Damage of bridges resulting from fault rupture in the 1999 Kocaeli and Duzce, Turkey earth-  
449 quakes and the 1999 Chi-Chi, Taiwan earthquake, *Structural Engineering/Earthquake Engineering*, 19(2),  
450 179s–197s, 2002.
- 451 Kelson, K. I., Kang, K. H., Page, W. D., Lee, C. T., and Cluff, L. S., 2001: Representative styles of deformation  
452 along the Chelungpu Fault from the 1999 Chi-Chi (Taiwan) earthquake: geomorphic characteristic and re-  
453 sponses of man-made structures, *Bull. Seismol. Soc. Am.*, 91(5), 930–952, 2001.
- 454 Kelson, K. I., Koehler, R. D., Kang, K.-H., Bray, J. D. and Cluff, L. S.: Surface deformation produced by the  
455 1999 Chi-chi (Taiwan) earthquake and interactions with built structures, Final Technical Report, U.S.G.S.  
456 Award No. 01-HQ-GR-0122, 21 pp., 2003.
- 457 Kerr, J., Nathan, S., Van Dissen, R., Webb, P., Brunndon, D., and King, A.: Planning for development of land on  
458 or close to active faults: A guide to assist resource management planners in New Zealand. Report prepared for  
459 the Ministry for the Environment by the Institute of Geological & Nuclear Sciences, Client Report 2002/124,  
460 Project Number 440W3301, 2003.
- 461 Konagai, K., Hori, M., Meguro, K., Koseki, J., Matsushima, T., Johansson, J., and Murata, O.: Key Points for Ra-  
462 tional Design for Civil Infrastructures near Seismic Faults Reflecting Soil-Structure Interaction Features, Re-  
463 port of JSPS research project, grant-in-aid for scientific research (A) Project No.16208048, 2006.
- 464 Kumahara, Y. and Nakata, T.: Recognition of active faults generating the 2005 Pakistan earthquake based on in-  
465 terpretation of the CORONA satellite photographs, *E-journal GEO*, 2 (2), 72-85, 2007 (In Japanese with Eng-  
466 lish abstract).
- 467 Lee, G. C. and Loh, C. H. (Eds): The Chi-Chi, Taiwan Earthquake of September 21, 1999: Reconnaissance Re-  
468 port, Technical Report MCEER-00-0003 April 30, 2000.
- 469 Lee, J. C. and Chan, Y. C.: Structure of the 1999 Chi-Chi earthquake rupture and interaction of thrust faults in the  
470 active fold belt of western Taiwan, *J. Asian Earth Sci.*, 31, 226-239, 2007.

- 471 Lee, J. C., Chen, Y. G., Sieh, K., Mueller, K., Chen, W. S., Chu, H. T., Chan, Y. C., Rubin, C., and Yeats, R.: A  
472 Vertical Exposure of the 1999 Surface Rupture of the Chelungpu Fault at Wufeng, Western Taiwan: Structural  
473 and Paleoseismic Implications for an Active Thrust Fault, *Bull. Seismol. Soc. Am.*, 91, 5, pp. 914-929,  
474 2001.
- 475 Lee, Y. H., Hsieh, M. L., Lu, S. D., Shih, T. S., Wu, W. Y., Sugiyama, Y., Azuma, T., and Kariya, Y.: Slip vec-  
476 tors of the surface rupture of the 1999 Chi-Chi earthquake, western Taiwan, *J. Struct. Geol.*, 25, 1917-1931,  
477 2003.
- 478 Lee, Y. H., Wu, K. C., Rau, R. J., Chen, H. C., Lo, W., and Cheng, K. C.: Revealing coseismic displacements and  
479 the deformation zones of the 1999 Chi-Chi earthquake in the Tsaotung area, central Taiwan, using digital ca-  
480 dastral data, *J. Geophys. Res.*, 115, B03419, 2010.
- 481 Lettis, W. R., Wells, D. L., and Baldwin, J. N.: Empirical observations regarding reverse earthquakes, blind  
482 thrust faults, and quaternary deformation: Are blind thrust faults truly blind?, *Bull. Seismol. Soc. Am.*, 87(5),  
483 1171–1198, 1997.
- 484 Lin, A., Sano, M., Yan, B., and Wang, M.: Co-seismic surface ruptures produced by the 2014 Mw 6.2 Nagano  
485 earthquake, along the Itoigawa–Shizuoka tectonic line, central Japan, *Tectonophysics*, 656, 142-153, 2015.
- 486 Lin, W. H.: On surface deformations from the Chi-Chi earthquake in the Shihkang and Chutzekeng areas, Special  
487 Issue for the Chi-Chi Earthquake, 1999, Special Publication of the Central Geological Survey, 12, 1-17, 2000  
488 (in Chinese with English abstract).
- 489 Liu-Zeng, J., Sun, J., Wang, P., Hudnut, K. W., Ji, C., Zhang, Z., Xu, Q., and Wen, L.: Surface ruptures on the  
490 transverse Xiaoyudong fault: A significant segment boundary breached during the 2008 Wenchuan earth-  
491 quake, China, *Tectonophysics* 580, 218–241, 2012.
- 492 Liu-Zeng, J., Sun, J., Zhang, Z., Wen, L., Xing, X., Hu, G., and Xu, Q.: Detailed mapping of surface rupture of  
493 the Wenchuan Ms 8.0 earthquake near Hongkou and seismotectonic implications, *Quaternary Sciences*, 30  
494 (1), 1-29, 2010 (in Chinese with English abstract).
- 495 Liu-Zeng, J., Zhang, Z., Wen, L., Tapponnier, P., Sun, J., Xing, X., Hu, G., Xu, Q., L. Zeng, L., Ding, L., Ji, C.,  
496 Hudnut, K.W., and van der Woerd, J.: Co-seismic ruptures of the 12 May 2008, Ms 8.0 Wenchuan earth-  
497 quake, Sichuan: East–west crustal shortening on oblique, parallel thrusts along the eastern edge of Tibet, *Earth  
498 Plan. Sci. Lett.*, 286, 355-370, 2009.
- 499 Machette, M. N., Crone, A. J., and Bowman, J. R.: Geologic investigations of the 1986 Marryat Creek, Australia,  
500 earthquakes - implications for paleoseismicity in stable continental regions, *U.S. Geol. Sur. Bull.* 2032-B, 29,  
501 1993.

- 502 McCaffrey, R.: Teleseismic investigation of the January 22, 1988 Tennant Creek, Australia, earthquakes, *Geophys. Res. Lett.*, 16, 413-416, 1989.
- 503
- 504 Meghraoui, M., Jaegy, R., Lammali, K., and Albarède, F.: Late Holocene earthquake sequences on the El Asnam  
505 (Algeria) thrust fault, *Earth Planet. Sci. Lett.*, 90, 187–203, 1988.
- 506 Okada, S., Ishimura, D., Niwa, Y., and Toda, S.: The First Surface-Rupturing Earthquake in 20 Years on a HERP  
507 Active Fault is Not Characteristic: The 2014 Mw 6.2 Nagano Event along the Northern Itoigawa–Shizuoka  
508 Tectonic Line, *Seismol. Res. Lett.*, 86 (5), 1–14, 2015.
- 509 Ota, Y., Huang, C. Y., Yuan, P. B., Sugiyama, Y., Lee, Y. H., Watanabe, M., Sawa, H., Yanagida, M., Sasaki, S.,  
510 Suzuki, Y., Tang, H. S., Shu, U.T., Yang, S. Y., Hirouchi, D., and Taniguchi, K.: Trenching Study at the  
511 Tsautun Site on the Central Part of The Chelungpu Fault, Taiwan, *J. Geogr.*, 110 (5), 698-707, 2001 (in Japa-  
512 nese with English abstract).
- 513 Ota, Y., Shishikura, M., Ichikawa, K., Watanabe, M., Yanagida, M., Tanaka, T., Sawa, H., Yamaguchi, M., Lee,  
514 Y. H., Lu, S. T., Shih, T. S., and Amagasa, S.: Low-angle reverse faulting during two earthquakes on the  
515 northern part of the Chelungpu fault, deduced from the Fengyuan trench, Central Taiwan, *Terr. Atmos.*  
516 *Ocean. Sci.*, v. 18, no. 1, p. 55–66, 2007b.
- 517 Ota, Y., Watanabe, M., Suzuki, Y., Yanagida, M., Miyawaki, A., and Sawa, H.: Style of the surface deformation  
518 by the 1999 Chichi earthquake at the central segment of Chelungpu fault, Taiwan, with special reference to  
519 the presence of the main and subsidiary faults and their progressive deformation in the Tsautun area, *J. Asian*  
520 *Earth Sci.*, 31, 214-225, 2007a.
- 521 Petersen, M., Dawson, T.E., Chen, R., Cao, T., Wills, C.J., Schwartz, D.P., and Frankel, A.D.: Fault displacement  
522 hazard for strike-slip faults, *Bull. Seismol. Soc. Am*, 101 (2), 805–825, 2011.
- 523 Philip, H. and Meghraoui, M.: Structural analysis and interpretation of the surface deformation of the El Asnam  
524 earthquake of October 10, 1980, *Tectonics*, 2, 17-49, 1983.
- 525 Philip, H., Rogozhin, E., Cisternas, A., Bousquet, J. C., Borisov, B., and Karakhanian, A.: The Armenian earth-  
526 quake of 1988 December 7: faulting and folding, neotectonics and palaeoseismicity, *Geophys. J. Int.*, 110,  
527 141-158, 1992.
- 528 Rajendran, C. P., Rajendran, K., Unnikrishnan, K. R., and John, B.: Palaeoseismic indicators in the rupture zone  
529 of the 1993 Killari (Latur) earthquake, *Curr. Sci.*, 70 (5), 385-390, 1996.
- 530 Rymer, M. J., Kendrick, K. J., Lienkaemper, J. J., and Clark, M. M.: Surface rupture on the Nunez fault during  
531 the Coalinga earthquake sequence, in Rymer, M.J, and Ellsworth, W.L. eds., *The Coalinga, California, Earth-*  
532 *quake of May 2, 1983*, U.S. Geol. Sur. Prof. Paper 1487, 299-318, 1990.

533 Sayab, M. and Khan, M.A.: Temporal evolution of surface rupture deduced from coseismic multi-mode second-  
534 ary fractures: Insights from the October 8, 2005 (Mw 7.6) Kashmir earthquake, NW Himalaya, *Tectonophys-*  
535 *ics*, 493, 58–73, 2010.

536 Seeber, L., Ekstrom, G., Jain, S.K., Murty, C.V.R., Chandak, N., and Armbruster, J. G.: The 1993 Killari earth-  
537 quake in central India: a new fault in Mesozoic basalt flows?, *J. Geophys. Res.*, 101, 8543-8560, 1996.

538 Shin, T. C. and Teng, T. L.: An overview of the 1999 Chi-Chi, Taiwan, Earthquake, Article in *Bull. Seismol.*  
539 *Soc. Am.*, 91(5), 895-913, 2001

540 SM Working Group: Guidelines for Seismic Microzonation, Conference of Regions and Autonomous Provinces  
541 of Italy, Civil Protection Department, English edition of: Gruppo di lavoro MS, Indirizzi e criteri per la micro-  
542 zonazione sismica, Conferenza delle Regioni e delle Province autonome – Dipartimento della protezione civi-  
543 le, Roma, 2008, 3 vol. e Dvd, 2015. Available online at  
544 [http://www.protezionecivile.gov.it/httpdocs/cms/attach\\_extra/GuidelinesForSeismicMicrozonation.pdf](http://www.protezionecivile.gov.it/httpdocs/cms/attach_extra/GuidelinesForSeismicMicrozonation.pdf), 2015.

545 Technical Commission for Seismic Microzonation: Linee guida per la gestione del territorio in aree interessate da  
546 Faglie Attive e Capaci (FAC), versione 1.0, Conferenza delle Regioni e delle Province Autonome – Diparti-  
547 mento della Protezione Civile, 55 pp., Roma, 2015 (In Italian).

548 Tsutsumi, H. and Yeats, R.: Tectonic setting of the 1971 Sylmar and 1994 Northridge earthquakes in the San  
549 Fernando valley, California, *Bull. Seism. Soc Am.*, 89 (5), 1232-1249, 1999.

550 U.S. Geological Survey Staff: Surface faulting, in: The San Fernando, California, earthquake of February 9,  
551 1971, *U.S. Geol. Sur. Prof. Paper 733*, 55-76, 1971.

552 Wang, H., Ran, Y, Chen, L., Shi, X., Liu, R., and Gomez, F.: Determination of horizontal shortening and amount  
553 of reverse-faulting from trenching across the surface rupture of the 2008 Mw 7.9 Wenchuan earthquake, Chi-  
554 na, *Tectonophysics*, 491, 10–20, 2010.

555 Wells, D. and Coppersmith, K.: New empirical relationships among magnitude, rupture length, rupture width,  
556 rupture area, and surface displacement, *Bull. Seismol. Soc. Am.*, 84 (4), 974-1002, 1994.

557 Wesnousky, S. G.: Displacement and geometrical characteristics of earthquake surface ruptures: Issues and im-  
558 plications for seismic hazard analysis and the earthquake rupture process, *Bull. Seismol. Soc. Am.*, 98(4),  
559 1609–1632, 2008.

560 Xu, X., Wen, X., Ye, J., Ma, B., Chen, J., Zhou, R., He, H., Tian, Q., He, Y., Wang, Z., Sun, Z., Feng, X., Yu, G.,  
561 Chen, L., Chen, G., Yu, S., Ran, Y., Li, X., Li, C., and An, Y.: The Ms 8.0 Wenchuan earthquake surface rup-  
562 tures and its seismogenic structure, *Seismol. Geol.*, 30 (3), 597-629, 2008 (in Chinese with English abstract).

563 Xu, X., Wen, X., Yu, G., Chen, G., Klinger, Y., Hubbard, J., and Shaw, J.: Co-seismic reverse- and oblique-slip  
564 surface faulting generated by the 2008 Mw 7.9 Wenchuan earthquake, China, *Geology* 37( 6), 515–518, doi  
565 10.1130/G25462A.1., 2009.

566 Yeats, R. S.: Active Faults Related to Folding, In *Active Tectonics: Impact on Society*, The National Academies  
567 Press, 280 pp., <https://doi.org/10.17226/624>, 1986.

568 Yelding, G., Jackson, J. A., King, G. C. P., Sinvhal H., Vita-Finzi, C., Wood, R. M.: Relations between surface  
569 deformation, fault geometry, seismicity, and rupture characteristics during the El Asnam (Algeria) earthquake  
570 of the 10 October 1980, *Earth Planet. Sci. Lett.*, 56, 287-304, 1981.

571 Youngs, Y., W. J. Arabasz, R. R., Anderson, R. E., Ramelli, A. R., Ake, J. P., Slemmons, D. B., McCalpin, J. P.,  
572 Doser, D. I., Fridrich, C. J., Swan III, F. H., Rogers, A. M., Yount, J. C., Anderson, L. W., Smith, K.  
573 D., Bruhn, R. L., Knuepfer, L. K., Smith, R. B., dePolo, C. M., O’Leary, K.W, Coppersmith, K. J., Pezzopane,  
574 S. K., Schwartz, D. P., Whitney, J. W., Olig, S. S., and Toro, G. R.: A methodology for probabilistic fault dis-  
575 placement hazard analysis (PFDHA), *Earthq. Spectra* 19, 191–219, 2003.

576 Yu, G. H., Xu, X. W., Chen, G. H., Gou, T. T., Tan, X. B., Yang, H., Gao, X., An, Y. F., and Yuan, R. M.: Rela-  
577 tionship between the localization of surface ruptures and building damages associated with the Wenchuan 8.0  
578 earthquake, *Chinese J. Geophysics*, Vol. 52, No. 6, pp. 1294-1311, 2009.

579 Yu, G., Xu, X., Klinger, Y., Diao, G., Chen, G., Feng, X., Li, C., Zhu, A., Yuan, R., Guo, T., Sun, X., Tan, X.,  
580 and An, Y.: Fault-Scarp Features and Cascading-Rupture Model for the Mw 7.9 Wenchuan Earthquake, East-  
581 ern Tibetan Plateau, China, *Bull. Seismol. Soc. Am.*, Vol. 100, No. 5B, pp. 2590-2614, 2010.

582 Zhang, J. Y., Bo, J. S., Xu, G. D., and Huang, J. Y.: Buildings Setbacks Research From Surface-Fault-Rupture  
583 Statistical Analysis, *Applied Mechanics and Materials*, Vols. 204-208, pp. 2410-2418, 2012.

584 Zhang, Y. S., Shi, J. S., Sun, P., Yang, W., Yao, X., Zhang, C. S., and Xiong T. Y.: Surface ruptures induced by  
585 the Wenchuan earthquake: Their influence widths and safety distances for construction sites, *Eng. Geol.* 166,  
586 245–254, 2013.

587 Zhang, Y. S., Sun, P., Shi, J. S., Yao, X., and Xiong, T. Y.: Investigation of rupture influenced zones and their  
588 corresponding safe distances for reconstruction after 5.12 Wenchuan earthquake, *Eng. Geol.*, 18 (3), 312-319,  
589 2010 (in Chinese with English abstract).

590 Zhou, Q., Xu, X., Yu, G., Chen, X., He, H., and Yin, G.: Width Distribution of the Surface Ruptures Associated  
591 with the Wenchuan Earthquake: Implication for the Setback Zone of the Seismogenic Faults in Post-  
592 earthquake Reconstruction, *Bull. Seismol. Soc. Am.*, Vol. 100, No. 5B, pp. 2660-2668, 2010.

593

**Table 1. Earthquakes used for analysing the width of the rupture zone (WRZ).**

Earthquake	Date	Magnitude	Kin. #	SRL* (km)	MD* (m)	Depth (km)	References for earthquake parameters (a) and WRZ calculation (b)
1) San Fernando, CA, USA	1971.02.09	M <sub>s</sub> 6.5, M <sub>w</sub> 6.6	R-LL	16	2.5	8.9 (USGS)	a) 1 b) 2
2) El Asnam, Algeria	1980.10.10	M <sub>s</sub> 7.3, M <sub>w</sub> 7.1	R	31	6.5	10 (USGS)	a) 1 b) 3, 4, 5
3) Coalinga (Nunez), CA, USA	1983.06.11	M <sub>s</sub> 5.4, M <sub>w</sub> 5.4	R	3.3	0.64	2.0 (USGS)	a) 1 b) 6
4) Marryat Creek, Australia	1986.03.30	M <sub>s</sub> 5.8, M <sub>w</sub> 5.8	R-LL	13	1.3	3.0	a) 1, 7 b) 8, 9
5) Tennant Creek, Australia	1988.01.22 (3 events)	M <sub>s</sub> 6.3, M <sub>w</sub> 6.3 M <sub>s</sub> 6.4, M <sub>w</sub> 6.4 M <sub>s</sub> 6.7, M <sub>w</sub> 6.6	R R-LL R	10.2 6.7 16	1.3 1.17 1.9	2.7 3.0 4.2	a) 1, 10 b) 11
6) Spitak, Armenia	1988.12.07	M <sub>s</sub> 6.8, M <sub>w</sub> 6.8	R-RL	25	2.0	5.0-7.0	a) 1, 12 b) 13
7) Killari, India	1993.09.29	M <sub>s</sub> 6.4, M <sub>w</sub> 6.2	R	5.5	0.5	2.6	a) 14, 15 b) 15, 16
8) Chi Chi, Taiwan	1999.09.20	M <sub>w</sub> 7.6	R-LL	72	12.7	8.0	a) 17, 18 b) 19, 20, 21, 22, 23, 24, 25, 26, 27, 28, 29, 30, 31, 32, 33, 34, 35, 36, 37, 38, 39, 40, 41
9) Kashmir, Pakistan	2005.10.08	M <sub>w</sub> 7.6	R	70	7.05 (v)	<15.0	a) 42, 43 b) 43, 44
10) Wenchuan, China	2008.05.12	M <sub>w</sub> 7.9	R-RL	240	6.5 (v) 4.9 (h)	19.0 (USGS)	a) 45 b) 46, 47, 48, 49, 50, 51, 52, 53, 54, 55, 56, 57, 58, 59
11) Nagano, Japan	2014.11.22	M <sub>w</sub> 6.2	R	9.3	1.5 (v)	4.5	a) 60, 62 b) 60, 61, 62

# Kin. (kinematics): R = reverse, LL = left lateral, RL = right lateral.

\* SRL = surface rupture length; MD = maximum displacement (vector sum, unless otherwise specified; v = vertical; h = horizontal).

References: 1 = Wells and Coppersmith, 1994; 2 = U.S. Geological Survey Staff, 1971; 3 = Yehling et al., 1981; 4 = Philip and Meghraoui, 1983; 5 = Meghraoui et al. 1988; 6 = Rymer et al. 1990; 7 = Fredrich et al., 1988; 8 = Bowman and Barlow, 1991; 9 = Machette et al., 1993; 10 = McCaffrey, 1989; 11 = Crone et al., 1992; 12 = Haessler et al. 1992; 13 = Philip et al. 1992; 14 = Lettis et al., 1997; 15 = Seeber et al. 1996; 16 = Rajendran et al., 1996; 17 = Wesnousky, 2008; 18 = Shin and Teng, 2001; 19 = Kelson et al., 2001; 20 = Kelson et al., 2003; 21 = Angelier et al., 2003; 22 = Bilham and Yu, 2000; 23 = Chang and Yang, 2004; 24 = Chen et al., 2000; 25 = Chen et al., 2003; 26 = Faccioli et al., 2008; 27 = Huang et al., 2008; 28 = Huang et al., 2000; 29 = Huang, 2006; 30 = Kawashima, 2002; 31 = Kona-gai et al., 2006; 32 = Lee and Loh, 2000; 33 = Lee et al., 2001; 34 = Lee and Chan, 2007; 35 = Lee et al., 2003; 36 = Lee et al., 2010; 37 = Lin, 2000; 38 = Ota et al., 2001; 39 = Ota et al., 2007a; 40 = Ota et al., 2007b; 41 = Central Geological Survey, MOEA at <http://gis.moeacgs.gov.tw/gwh/gsb97-1/sys8/index.cfm>; 42 = Avouac et al., 2006; 43 = Kaneda et al., 2008; 44 = Kumahara and Nakata, 2007; 45 = Xu et al., 2009; 46 = Liu-Zeng et al., 2009; 47 = Liu-Zeng et al., 2012; 48 = Yu et al., 2009; 49 = Yu et al., 2010; 50 = Zhou et al., 2010; 51 = Zhang et al., 2013; 52 = Chen et al., 2008; 53 = Dong et al., 2008a; 54 = Dong et al., 2008b; 55 = Liu-Zeng et al., 2010; 56 = Wang et al., 2010; 57 = Xu et al., 2008; 58 = Zhang et al., 2012; 59 = Zhang et al., 2010; 60 = Okada et al., 2015; 61 = Ishimura et al., 2015; 62 = Lin et al., 2015.

612 **Table 2 - Width of the rupture zone (WRZ) on the hanging wall (HW) and on the footwall (FW) and FW to HW ratio**  
 613 **for (a) “simple thrust” distributed ruptures (B-M, F-S and Sy excluded) and (b) all distributed ruptures.**

614

615 (a)

616 <b>Probability<sup>1</sup></b>	<b>WRZ HW</b>	<b>WRZ FW</b>	<b>Total WRZ</b>	<b>FW:HW</b>
617 90%	575 m	265 m	840 m	1:2.2
618 75%	260 m	120 m	380 m	1:2.2
619 50%	80 m	45 m	125 m	1:1.8
620 35% <sup>2</sup>	40 m	20 m	60 m	1:2

625 (b)

626 <b>Probability<sup>1</sup></b>	<b>WRZ HW</b>	<b>WRZ FW</b>	<b>Total WRZ</b>	<b>FW:HW</b>
627 90%	1100 m	720 m	1820 m	1:1.5
628 75%	640 m	330 m	970 m	1:1.9
629 50%	260 m	125 m	385 m	1:2.1
630 35% <sup>3</sup>	130 m	65 m	195 m	1:2

636 <sup>1</sup> Probabilities refer to the cumulative distribution functions of Fig.s 4 and 5.

637 <sup>2</sup> Corresponding to a sharp drop of data in the histograms of Fig. 4, close to the principal fault.

638 <sup>3</sup> Calculated for comparison with “simple thrust” database, but not corresponding to particular drops of data in the histo-  
 639 grams of Fig. 5.

640

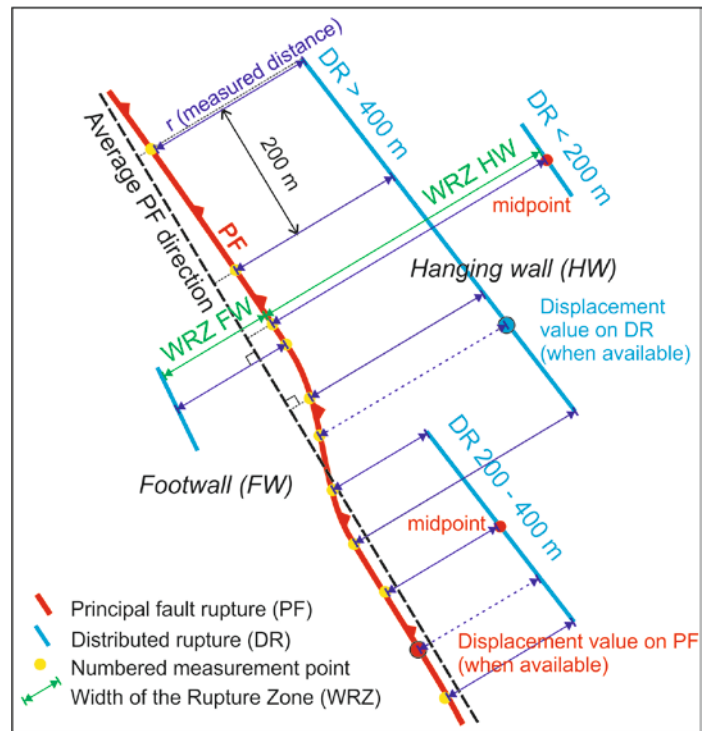
641 **Table 3 Comparison between fault zone size from Italian guidelines and the Width of the Rupture Zone (WRZ) from**  
 642 **the present study (proposal for integrating fault zoning for thrust faults). PF = principal fault rupture; DR = distrib-**  
 643 **uted ruptures; SFRH = surface fault rupture hazard.**

<b>ZONE<sup>1</sup></b>	<b>Seismic Microzonation<sup>2</sup></b>	<b>Italian guidelines</b>	<b>Proposed widths of zones from total WRZ (from “simple thrust” DR<sup>3</sup>)</b>	<b>Total WRZ from all DR (including B-M, F-S and Sy)</b>	<b>FW:HW<sup>5</sup></b>
Warning Zone ( <i>Zona di attenzione, ZA</i> )	Basic (Level 1)	400 m  (FW:HW = 1:2)	<b>&gt; 380 m</b> (minimum; 75% prob.)  <b>to 840 m</b> (recommended; 90% prob., all the reasonably inferred hazard from PF and DR)	<b>1800 m</b> (90% prob., applicable in poorly-known areas for assessing the extent of potential SFRH)	1:2
Avoidance Zone ( <i>Zona di rispetto, ZR</i> )	High-level (Level 3)	30 m  (FW:HW = 1:2)	<b>60 m</b> (35% prob. <sup>4</sup> , very high hazard)		1:2
Susceptible Zone ( <i>Zona di suscettibilità, ZS</i> )	High-level (Level 3)	160 m  (FW:HW = 1:2)	<b>Variable</b> (depending on the detail of Level 3 MS and structural complexity)  <b>380 m</b> (in the absence of particular constraints; 75% prob., precautionary)		1:2

644  
 645 <sup>1</sup> The original names of zones in the Italian guidelines (in Italian) are in italics.  
 646 <sup>2</sup> Different levels of Seismic Microzonation refer to SM Working Group (2015).  
 647 <sup>3</sup> B-M, F-S and Sy fault ruptures are not included.  
 648 <sup>4</sup> Corresponding to a sharp drop of data in the histograms of Fig. 4.  
 649 <sup>5</sup> The computed values (Table 2) have been simplified to 1:2.  
 650

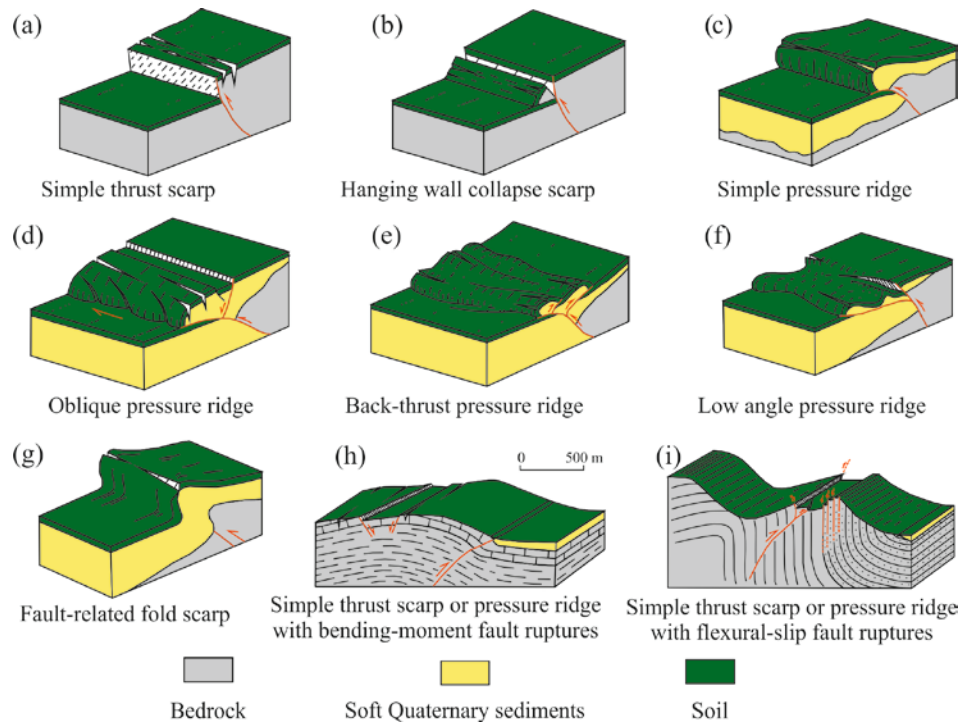
651  
652  
653  
654  
655  
656  
657  
658  
659  
660

Figure 1 Sketch synthesizing the methodology used for measuring the “r” and WRZ data. Distance between the principal fault rupture and distributed rupture is measured along the line perpendicular to the auxiliary line indicating the average direction of the principal fault, always between the faults. Points with displacement values are prioritised at the expense of the 200 m metrics (the closest measurement point) when reasonable, in order to avoid over measuring.



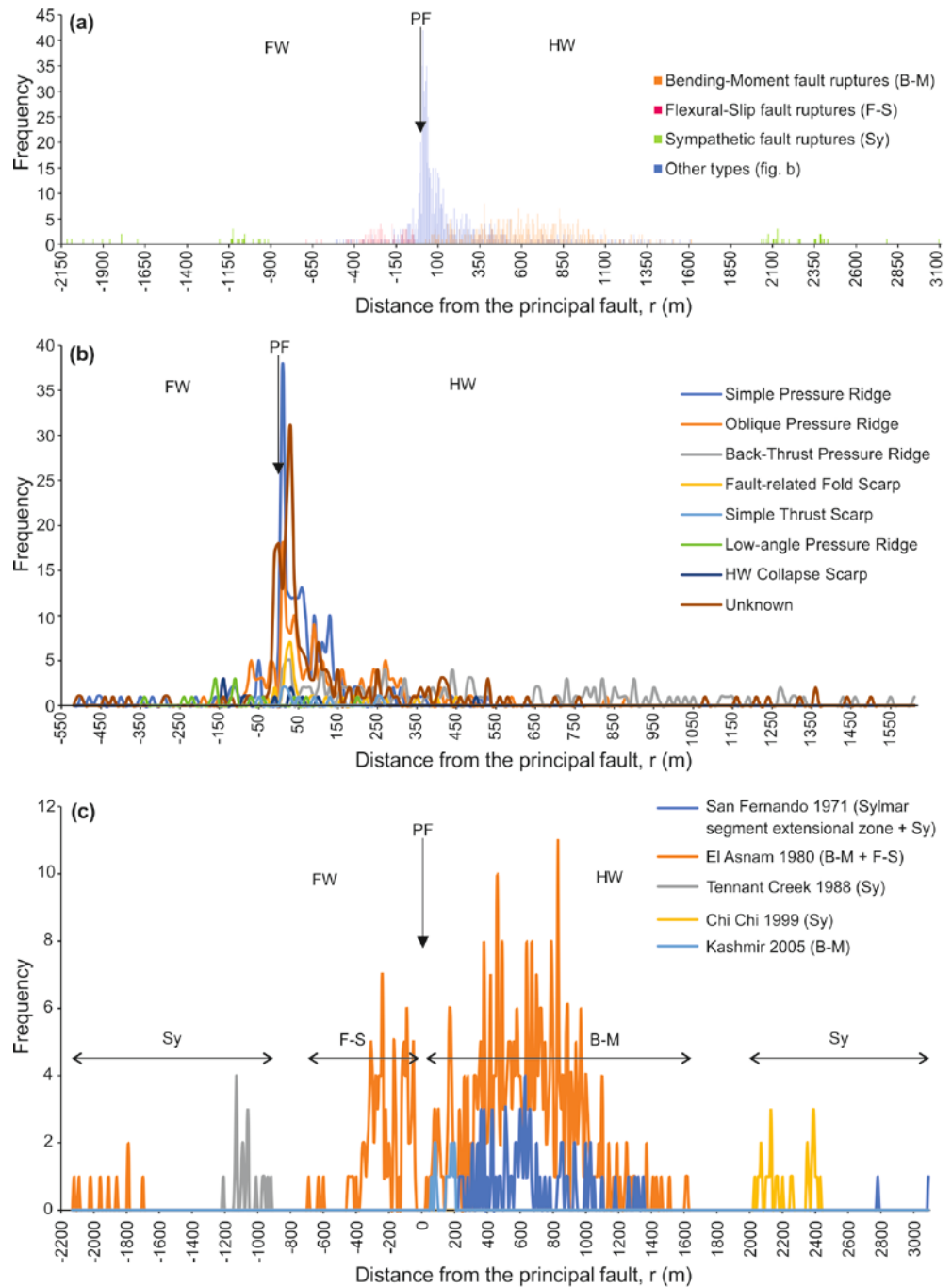
661  
662  
663  
664  
665  
666  
667  
668  
669

Figure 2 Scarp type classification (modified after Philip et al., 1992 and Yu et al., 2010). The scarp types h) and i) are associated with large-scale folds (hundreds of meters to kilometres in wavelength) and are from Philip and Meghraoui (1983).



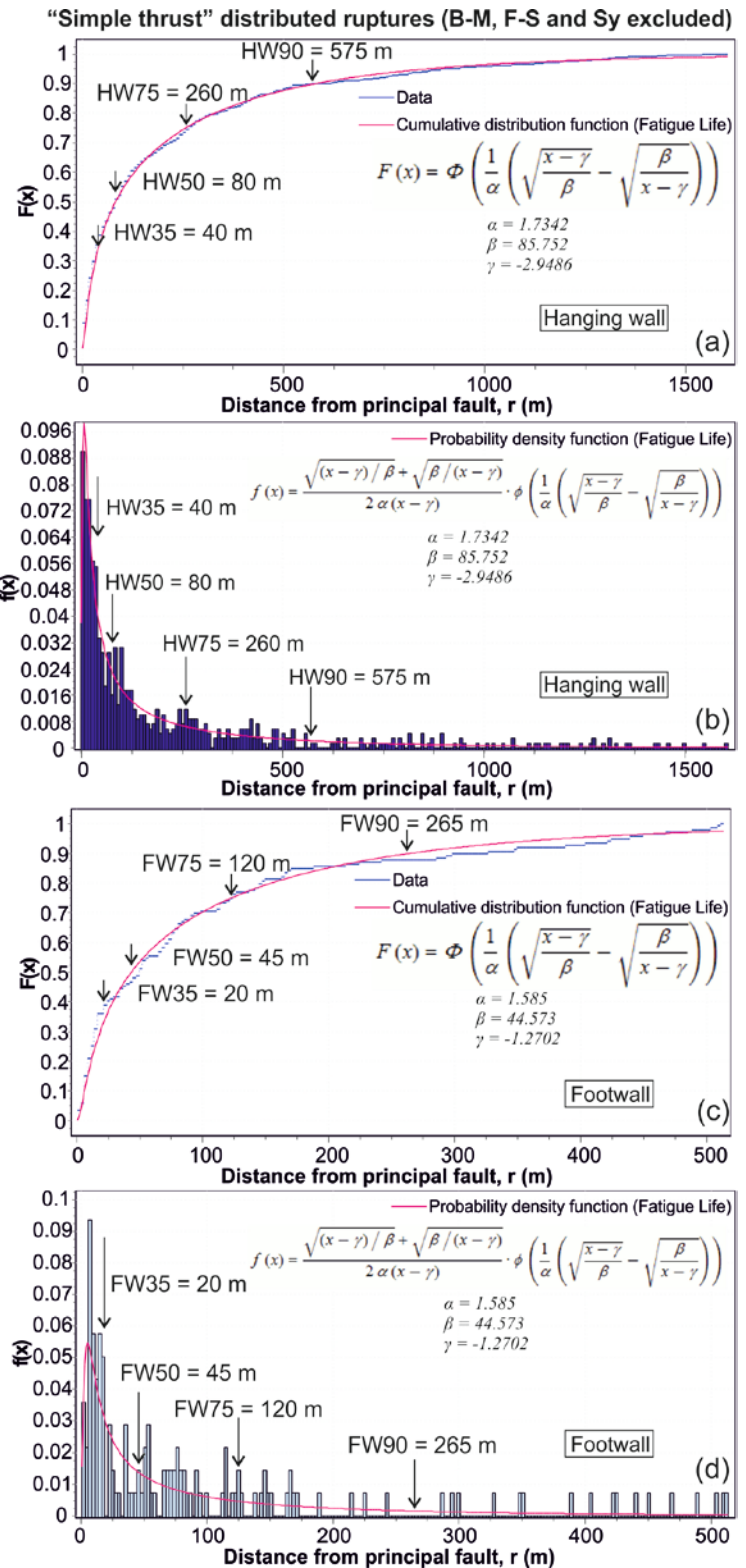
670  
 671  
 672  
 673  
 674  
 675  
 676  
 677  
 678  
 679  
 680  
 681  
 682  
 683  
 684  
 685  
 686  
 687  
 688  
 689  
 690  
 691  
 692  
 693  
 694

Figure 3 a) Frequency distribution histogram of the distributed ruptures distance ( $r$ ) from the principal fault rupture (PF) for the earthquakes reported in Table 1. The positive and negative values refer to the data on the hanging wall and the footwall, respectively; b) Frequency distribution curves of each scarp type excluding those associated with B-M, F-S and Sy fault ruptures (types h and i of Fig. 2 and sympathetic slip triggered on distant faults); c) Frequency distribution curves of the B-M, F-S and Sy fault ruptures distinguished by earthquakes (the Sylmar segment extensional zone of the San Fernando 1971 earthquake rupture is included into the B-M fault ruptures).



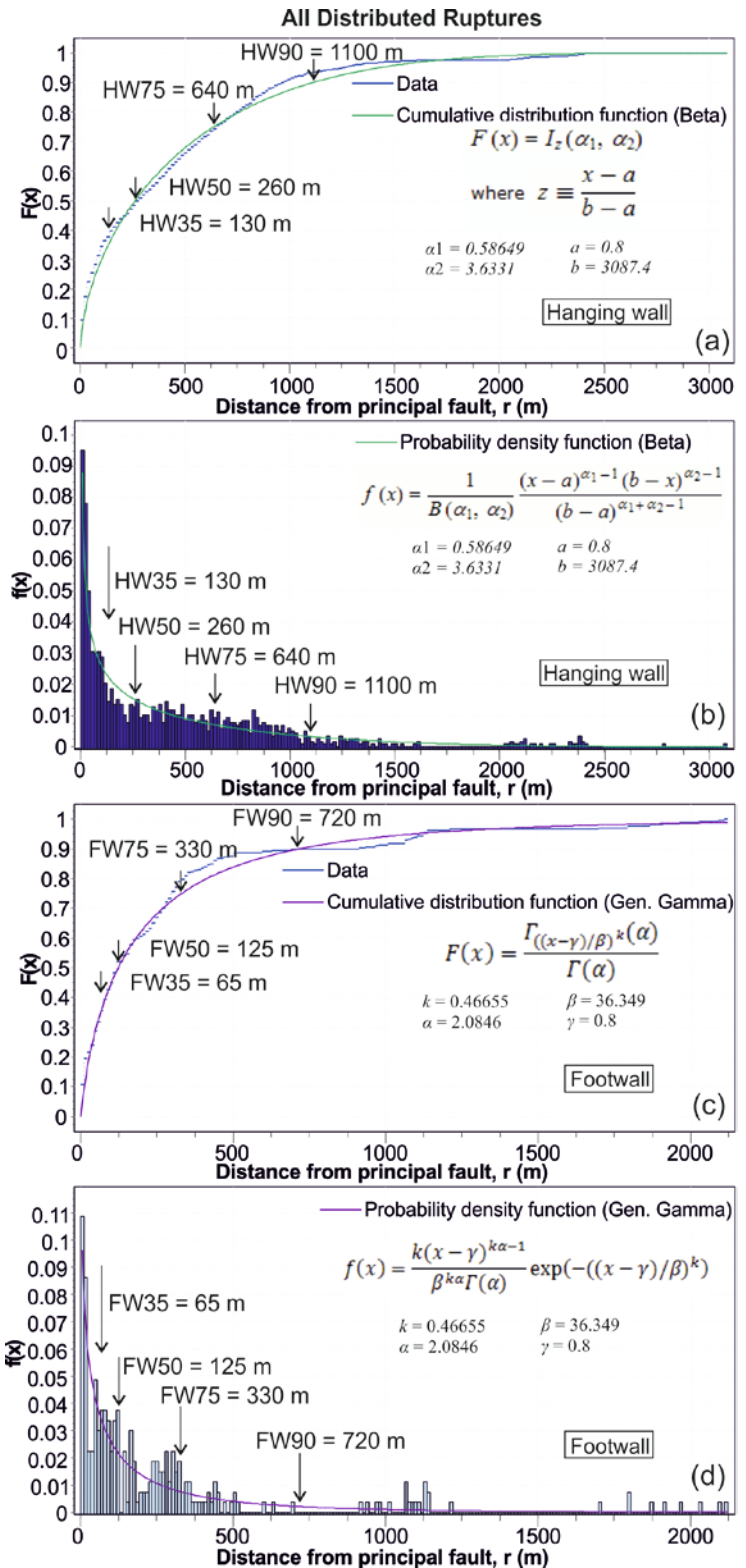
695  
696  
697  
698  
699  
700  
701  
702  
703  
704

Figure 4 Cumulative distribution function and probability density function of the rupture distance (r) from the PF for the hanging wall (a and b, respectively) and the footwall (b and c, respectively) of the PF. Only the scarp types without associated B-M, F-S or sympathetic fault ruptures (“simple thrust” distributed ruptures) were analysed. The 35% probability (HW35) is indicated because it corresponds to a sharp drop of the data in the histograms.



705  
706  
707  
708  
709  
710  
711  
712  
713  
714

Figure 5 Cumulative distribution function and probability density function of the rupture distance (r) from the PF for the hanging wall (a and b, respectively) and the footwall (c and d, respectively) of the PF. All types of distributed ruptures were considered. The 35% probability (HW35) is indicated for comparison with “simple thrust” database (Fig. 4), but it does not correspond to particular drops of the data in the histograms.



715

716 Figure 6 a) Diagram plotting the total  
717 WRZ (WRZ<sub>tot</sub> = WRZ hanging wall +  
718 WRZ footwall) against (a) the earth-  
719 quake magnitude ( $M_w$ ) and (b) the ver-  
720 tical displacement (VD) on the princi-  
721 pal fault.

